Preparation, Thermal and Mechanical Properties of POSS Epoxy Hybrid Composites

Fei Xiao, Yangyang Sun, Yonghao Xiu, C. P. Wong

School of Materials Science and Engineering, Georgia Institute of Technology, Atlanta, Georgia 30332

Received 21 September 2006; accepted 27 October 2006
DOI 10.1002/app.25746
Published online 7 February 2007 in Wiley InterScience (www.interscience.wiley.com).

ABSTRACT: Polyhedral oligomeric silsesquioxanes (POSS) epoxy hybrid composites have attracted much research interest because of their unique structure, versatile synthetic approaches, and changeable properties through molecular tailoring. Octakis(dimethylsiloxypropylglycidyl ether)silsesquioxane and octakis(dimethylsiloxyethylcyclohexenyl epoxide)silsesquioxane were synthesized and cured with 4,4′-methylenebis(cyclohexylamine) and 4-methylhexahydrophthalic anhydride to prepare the highly crosslinked hybrid materials. The thermochemical data from DSC analysis and FTIR show that the curing reactions of POSS epoxy are more difficult than diglycidyl ether of bisphenol A (DGEBA) resin because of steric hindrance. The multifunctional structure of POSS can form highly crosslinked network throughout the composites, therefore the polymer main framework is frozen and cannot move freely. Some POSS composites do not show glass transitions and the observed relaxation for other POSS composites is likely due to the motion of tethers between POSS cores. The moduli of POSS composites, which decrease slowly with temperature increasing, are much higher than that of DGEBA resins at high temperatures. Although the coefficients of thermal expansion of POSS composites are larger than that of DGEBA resins at low temperatures, they are less dependent on temperature and relatively low at high temperatures. The unique thermal and mechanical properties of POSS composites make them potential candidates for applications in high temperature and temperature variable environments. © 2007 Wiley Periodicals, Inc. J Appl Polym Sci 104: 2113–2121, 2007

Key words: polyhedral oligomeric silsesquioxanes; epoxy; nanocomposites; thermal properties; mechanical properties

INTRODUCTION

Silica-epoxy composites, with advantages of good adhesive ability, processibility, low polymer cost, and the low coefficients of thermal expansion (CTE), and high modulus of silica, have been applied widely in electronic packaging, such as molding compounds and underfills.[1,2] With increasing filler loading and decreasing filler size, the filler-epoxy interfaces increase and greatly impact the composites properties. The issue is extremely severe for nano-sized filler, for which a filler surface modification is needed to reduce the effect of interfaces. On the other hand, organic–inorganic hybrid composites with molecular level mixing eliminate the interface between the inorganic filler and organic matrix, affording an efficient way to solve the problems associated with the interface. Polyhedral oligomeric silsesquioxanes (POSS) are an interesting class of three-dimensional silsesquioxanes, which represent a soluble model for silica. Among them, octasilsesquioxanes attract more attention because of their unique cubic-like structure shown in Figure 1 and the simple synthesis process.[3]

POSS compounds are synthesized from hydrolytic condensation of silicates. Most of the reactions give very low yields of pure POSS (less than 10%), which limits the application of POSS. Octakis(dimethylsiloxyl)silsesquioxane ($Q_8M_8^H$) is one of the few POSS compounds that can be synthesized by hydrolytic condensation of simple silicates followed by silylation in high yield.[4] Further functionalization of $Q_8M_8^H$ is readily achieved through hydrosilylations. Various polymerizable functional groups, including epoxy,[5–7] isocyanate,[8] methacrylate,[9] and benzoxazine,[10] have been grafted on the eight vertexes of POSS in this way, which makes POSS nano building blocks for various polymeric hybrid materials. Laine and coworker synthesized two epoxy substituted POSS derivatives, octakis(dimethylsiloxypropylglycidyl ether)silsesquioxane (OG)[5] and octakis(dimethylsiloxyethylcyclohexenyl epoxide)silsesquioxane (OC),[11] and prepared POSS composites with diaminodiphenylmethane (DDM) as hardener and investigated the structure and properties of the composites.[11,12] Chen et al. studied the curing kinetics of OG and *meta*-phenylenediamine (*m*PDA), thermal and dielectric properties of the composite.[13] OG and OC have been incorporated into polyimides to improve the dielectric and thermomechanical properties of the materials.[14,15] Recently POSS epoxy composites made of octakis (aminophenyl)silsesquioxane (OAPS) were reported to show very low CTE.[16]

Correspondence to: C. P. Wong (cp.wong@mse.gatech.edu).

© 2007 Wiley Periodicals, Inc.

WILEY InterScience® DISCOVER SOMETHING GREAT

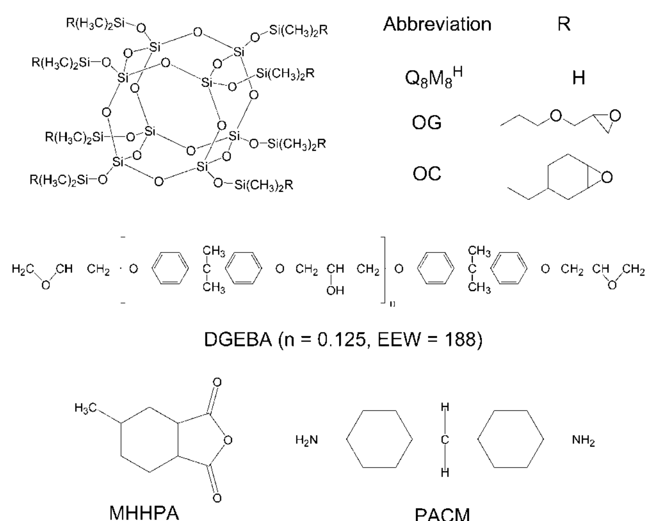

Figure 1 Molecular structures of POSS derivatives, DGEBA, and hardeners.

Octasilsesquioxane macromonomers can form highly crosslinked networks through their eight functional groups and exhibit unique thermal and mechanical characteristics. The potential application of POSS composites in electronic packaging promotes us to further investigate their thermal and mechanical properties, and their relationship to structure. In the above-mentioned studies, aromatic amines were used as hardener, which are less reactive toward epoxy, especially the secondary aromatic amine. Hence, the unreacted epoxy groups in stoichiometric samples may cause defects in the sample and affect the final properties of the composite. Aliphatic amine and anhydride, such as 4,4′-methylenebis(cyclohexylamine) (PACM) and 4-methylhexahydrophthalic anhydride (MHHPA), are more reactive toward epoxies than aromatic amines. Furthermore, their liquid character causes less viscosity problems from a processing point of view and is important for applications in electronic packaging. In this article, we reported the preparation of POSS epoxy hybrid composites using PACM and MHHPA as hardeners and the unusual thermomechanical properties of the composites.

EXPERIMENTAL

Materials

Diglycidyl ether of bisphenol A (DGEBA, EPON-828) was purchased from Miller-Stephenson Chemical (Danbury, CT). 4-Methylhexahydrophthalic anhydride (MHHPA) was supplied by Lindau Chemicals (Columbia, SC). 2-Ethyl-4-methyl-1H-imidazole-1-propanenitrile (2E4MZ-CN) was supplied by Shikoku Chemical Corp. (Kagawa, Japan). 4,4′-Methylenebis-(cyclohexylamine) (PACM) was obtained from Air Products and Chemicals (Allentown, PA). Tetraethyl orthosilicate (TEOS), tetramethylammonium hydroxide solution (25 wt % in methanol), allyl glycidyl ether, and 4-vinyl-1-cyclohexene 1,2-epoxide (mixture of isomers) were purchased from Aldrich. Platinum divinyltetramethyldisiloxane complex was purchased from United Chemical Technologies (Bristol, PA). Dimethyl chlorosilane was purchased from Gelest (Morrisville, PA).

Syntheses of POSS derivatives

Octakis(dimethylsiloxyl)silsesquioxane

Octakis(dimethylsiloxyl)silsesquioxane ($Q_8M_8^H$) was synthesized from TEOS with a yield of 87% in a similar method to the literature.[5] ^{1}H-NMR ($CDCl_3$, ppm): 4.71 (septet, $J = 2.8$ Hz, 8H), 0.23 (d, $J = 2.8$ Hz, 48H). ^{13}C-NMR ($CDCl_3$, ppm): 0.05. FTIR (KBr, cm^{-1}): 2965, 2144, 1257, 1101, 903, 838, 772, 555.

Octakis(dimethylsiloxypropylglycidyl ether)silsesquioxane[5]

$Q_8M_8^H$ (3.49 g, 3.43 mmol) and allyl glycidyl ether (3.44 g, 30.2 mmol) were dissolved in toluene (30 mL) with stirring in a flask flushed and kept in nitrogen at 50°C. Platinum divinyltetramethyldisiloxane in toluene (0.01*M*, 1.5 mL) was added and mixture was stirred at 50°C for 30 h. After removal of toluene on a rotary evaporator, the residue was dried in a vacuum oven at 90°C for 2 h. Octakis(dimethylsiloxypropylglycidyl ether)silsesquioxane (OG) was obtained as opaque viscous liquid (6.30 g, 95% based on $Q_8M_8^H$). ^{1}H-NMR ($CDCl_3$, ppm): 3.69–3.65 (dd, J = 11.5, 3.0 Hz, OCH_2C epoxide, 8H), 3.45–3.40 (m, OCH_2, 16H), 3.37–3.33 (dd, J = 11.5, 5.8 Hz, OCH_2C epoxide, 8H), 3.11 (t, J = 2.8 Hz, epoxide CH, 8H), 2.77 (t, J = 4.4 Hz, epoxide CH_2, 8H), 2.59–2.33 (dd, J = 4.9, 2.6 Hz, epoxide CH_2, 8H), 1.63–1.57 (m, Si-C-CH_2, 16H), 0.60–0.56 (m, SiCH_2, 16H), 0.12 (S, $SiCH_3$, 48H). ^{13}C-NMR ($CDCl_3$, ppm): 74.1, 71.4 (ether CH_2OCH_2), 50.8 (epoxide CH), 44.3 (epoxide CH_2), 23.1 (Si-C-CH_2), 13.6 ($SiCH_2$), −0.4 (Si—CH_3). FTIR (NaCl, cm^{-1}): 3057, 2997, 2957, 2932, 2871, 1254, 1169, 1093, 910, 845, 781.

Octakis(dimethylsiloxyethylcyclohexenyl epoxide)silsesquioxane[11]

$Q_8M_8^H$ (3.05 g, 3.00 mmol) and 4-vinyl-1-cyclohexene 1,2-epoxide (3.24 g, 26.1 mmol) were dissolved in toluene (30 mL) with stirring in a flask flushed and kept in nitrogen at 50°C. Platinum divinyltetramethyldisiloxane in toluene (0.01*M*, 1.5 mL) was added and mixture was stirred at 50°C for 20 h. After removal of toluene on a rotary evaporator, the residue was dried in a vacuum oven at 90°C for 2 h. Octakis(dimethylsiloxyethylcyclohexenyl epoxide)silsesquioxane (OC) was obtained as white solid after cooling (5.82 g, 96%

based on $Q_8M_8^H$). ^{1}H-NMR ($CDCl_3$, ppm): 3.13, 3.11 (s+s, 16H, epoxide CH), 2.13 (t, J = 13.7 Hz, 8H), 2.05–1.93 (m, 8H), 1.83–1.75 (m, 4H), 1.71–1.63 (m, 4H), 1.50–1.46 (m, 4H), 1.39–0.96 (m, 40H), 0.91–0.80 (m, 4H), 0.54–0.48 (m, 16H, Si—CH_2), 0.09 (s, 48H, Si—CH_3); ^{13}C-NMR ($CDCl_3$, ppm): 53.2, 52.7, 51.9, 51.8 (epoxide CH), 35.3, 32.2, 31.5, 30.4, 29.8, 29.2, 26.7, 25.4, 24.0, 23.6 (cyclohexyl and Si—CH_2CH_2), 14.5, 14.4 (Si—CH_2CH_2), −0.4 (Si—CH_3). FTIR (KBr, cm^{-1}): 2989, 2918, 2850, 1253, 1173, 1096, 886, 848, 794, 555.

Sample preparation

For stoichiometric curing reactions, the molar ratio of epoxy ring to NH_2 is 2 : 1. Because the reaction between epoxy and secondary amine is sterically hindered and much slower than primary amine, the molar ratio of 1 : 1 was also used. The sample differences are denoted by the suffix of abbreviation. For example, DGEBA-PACM-21 and DGEBA-PACM-11 would indicate the DGEBA epoxy cured by stoichiometric and double stoichiometric amount of PACM, respectively. And for better performance of anhydride cured epoxy, 1 : 0.85 epoxy/anhydride molar ratio was used and 1 wt % of 2E4MZ-CN was added before curing as accelerator. The liquid epoxy (DGEBA and OG) was mixed with PACM or MHHPA before curing. OC can be mixed with PACM or MHHPA at elevated temperature to give a viscous liquid. The curing conditions were determined from the dynamic DSC profile and listed in Table I.

TABLE I
Curing Conditions for the Composites

Sample	Condition
DGEBA-PACM-21	2 h at 80°C and 2 h at 150°C
DGEBA-PACM-11	2 h at 80°C and 2 h at 150°C
DGEBA-MHHPA	2 h at 165°C
OG-PACM-21	2 h at 80°C, 2 h at 150°C, and 1 h at 200°C
OG-PACM-11	2 h at 80°C and 2 h at 150°C
OG-MHHPA	2 h at 165°C
OC-PACM-21	2 h at 100°C, 2 h at 150°C, and 2 h at 220°C
OC-PACM-11	2 h at 100°C, 2 h at 150°C, and 2 h at 220°C
OC-MHHPA	1 h at 100°C and 2 h at 210°C

Characterizations

NMR analyses

^{1}H- and ^{13}C-NMR analyses were performed with a Bruker AMX 400 spectrometer at 400.137 and 100.623 MHz, respectively. $CDCl_3$ was used as solvent with the residue $CDCl_3$ signals as internal references at 7.24 and 77.0 ppm, respectively.

Fourier transform infrared spectroscopy

Fourier transform infrared (FTIR) spectra were obtained on Nicolet Magna 560 FTIR spectrometer operating at a resolution of 4 cm^{-1}. The liquid samples were measured in thin film between two NaCl crystal windows. The solid samples were grounded together with KBr powder and then pressed to a pellet.

Modulated differential scanning calorimetry

The curing behavior of epoxy was measured using a TA 2920 modulated differential scanning calorimeter (MDSC) operating under nitrogen atmosphere. An exactly weighed sample (∼10 mg) was placed in a hermetically sealed aluminum pan and heated from room temperature to 300°C at a ramping rate of 5°C/min in the DSC cell. The sample was then cooled to room temperature and rescanned from 25 to 250°C at a ramping rate of 5°C/min using an amplitude of modulation of ±0.5°C and a period of 40 s. The glass transition temperature (T_g) was obtained from step temperature in reverse heat flow curve.

Thermal gravimetric analysis

Thermal stability of cured epoxy samples under nitrogen were examined using a thermal gravimetric analyzer (model 2050, TA Instruments). Sample (10–20 mg) was loaded in a Platinum pan and heated from room temperature to 800°C at a ramping rate of 5°C/min. The N_2 flow rate was 77 mL/min.

Dynamic mechanical analysis

The dynamic mechanical properties of the materials were evaluated using a dynamic mechanical analyzer (model 2980, TA Instruments). The cured samples were cut and polished to a strip (∼10 × 6 × 3 mm^3). The tests were performed in a single-cantilever mode from 30 to 200°C at a ramping rate of 5°C/min. The amplitude applied to the samples in the experiments was 15 μm at a frequency of 1 Hz and resulted in a strain level of around 0.5%, which was within the linear viscoelastic region of the epoxy.

Thermomechanical analysis

The CTE of the cured samples were measured on a thermomechanical analyzer (model 2940, TA Instruments) under N_2. The dimensions of the samples were about 5 × 5 × 3 mm^3. The sample was heated in the thermomechanical analysis (TMA) furnace from room temperature to 200°C at a ramping rate of 5°C/min with a force of 0.05N.

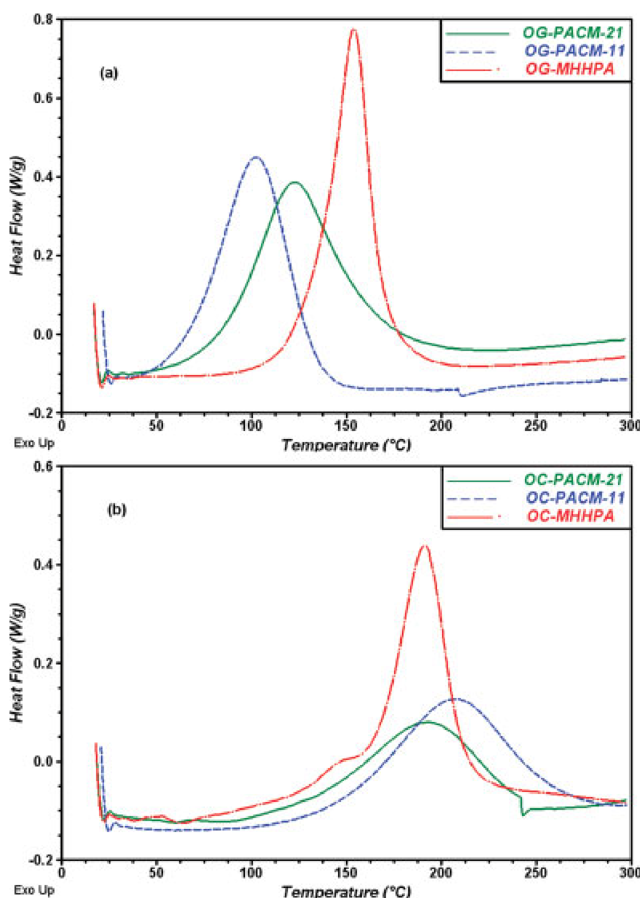

Figure 2 Dynamic DSC profile (a) OG composites, (b) OC composites. [Color figure can be viewed in the online issue, which is available at www.interscience.wiley.com.]

RESULTS AND DISCUSSION

Preparation of composites

Figure 1 shows the molecular structure of POSS derivatives, DGEBA, and hardeners. As each amine group (NH_2) can react with two epoxy groups theoretically, the 2 : 1 epoxy/amine molar ratio is preferred. Considering the curing reaction of secondary amine is sterically hindered, the composites with 1 : 1 epoxy/amine molar ratio were also prepared for comparison. The composites were synthesized by mixing equivalent quantities of epoxy and hardener, and curing at appropriate temperature determined from DSC measurement.

Figure 2 shows the curing profiles of the POSS composites measured by DSC. The exothermal peak temperature and integrated peak obtained from the profile are summarized in Table II. Supposing the epoxy rings in the formulation are completely consumed in the curing process, the molar reaction heats for epoxy are calculated from the integration values and the epoxy contents. The molar epoxy reaction heat for most of the reactions are about 100–120 kJ/mol. A slightly lower reaction heat for DGEBA curing with stoichiometric amount of PACM is attributed to the steric hindrance that prevents the approach of the secondary amine group to epoxy when most of the crosslinking was established in the resin.

OG has the same glycidyl group as DGEBA and exhibited similar reactivity to DGEBA, as shown from the exotherm, onset point, and reaction heat. The number of epoxy rings in OG is four times that of DGEBA, therefore more steric hindrance was expected and a lower heat of reaction OG-PACM-21 was observed. The onset temperature of the curing reaction, which corresponds to the start point of reaction between primary amine and epoxy, is not dependent on the epoxy/amine molar ratio. However, the end point is influenced by the epoxy/amine molar ratio. The OG-PACM-11 curing reaction ended below 150°C, whereas OG-PACM-21curing profile showed a much wide peak and curing continued to temperatures higher than 200°C because of the difficulty of the reaction between epoxy and secondary amine.

OC has sterically hindered epoxy groups and a rigid cyclic structure. The curing reaction occurred at much higher temperatures than OG and the curing profiles showed wide peaks. When PACM was used as hardener, the OC curing reaction is difficult to complete as indicated by the reaction heat. Supposing the reaction heat of the epoxy ring is 110 kJ/mol, then the conversions of epoxy in OG-PACM-21, OC-PACM-21, and OC-PACM-11 in DSC measurements are estimated to be only 80, 50, and 80%, respectively. To ensure that most epoxy groups on POSS react with

TABLE II
Curing Characteristics of POSS Composites

Sample	Exotherm (°C)	Integration (J/g)	Reaction heat (kJ/mol)
DGEBA-PACM-21	99	436	105
DGEBA-PACM-11	98	398	117
DGEBA-MHHPA	144	334	111
OG-PACM-21	123	309	91
OG-PACM-11	103	304	105
OG-MHHPA	154	298	116
OC-PACM-21	192	174	53
OC-PACM-11	213	244	89
OC-MHHPA	191	263	104

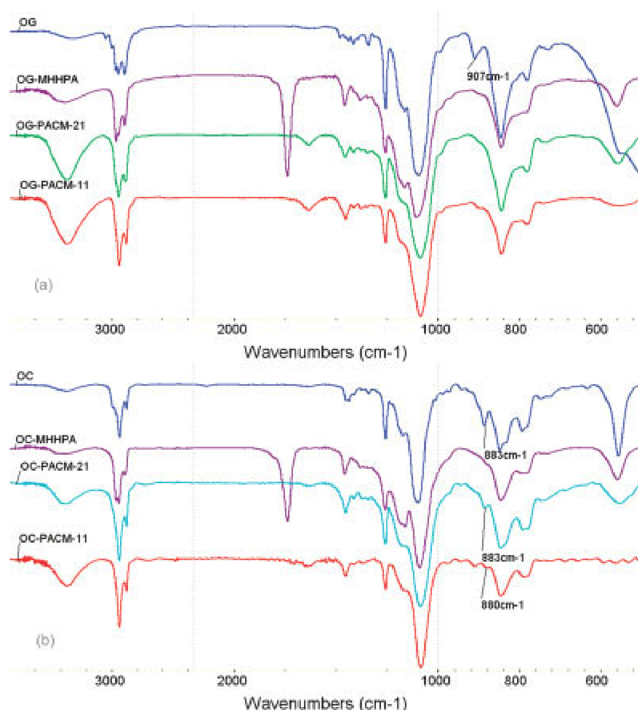

Figure 3 FTIR spectra of POSS composites (a) OG, (b) OC. [Color figure can be viewed in the online issue, which is available at www.interscience.wiley.com.]

hardener, the preparation of POSS composites were carried out at the temperatures of at least 10 degrees higher than the peak temperature in DSC profile.

The curing process of POSS composites were further studied by FTIR, as shown in Figure 3. Although high temperatures (>200°C) were used in curing reactions, FTIR spectra revealed that the OC composites were still not fully cured with PACM. The stretching vibration band of epoxy ring in OC appears at 883 cm^{-1}. After curing with PACM, the residual epoxy peak can be found at 883–880 cm^{-1} for OC-PACM-21 and OC-PACM-11. The strength of the residual epoxy peak decreased with the increasing PACM concentrations in the sample formulation. The epoxy ring's stretching vibration in OG absorbs at 907 cm^{-1} however, the residual epoxy peak in cured OG samples is not obvious. The reason is that the reactivity of the epoxy ring in OG is higher than that in OC, the curing reaction of OG is nearly complete.

It was reported that the epoxy groups in OG were difficult to cure completely by *m*PDA and unreacted epoxy signal could be found even after postcuring at 190°C for 3 h.[13] PACM is more reactive and flexible than *m*PDA and 4,4′-DDM, therefore cures better with OG composites.

Thermal stability of the composites

The thermal stabilities of the composites were analyzed by thermal gravimetric analysis (TGA). The initial mass loss temperatures (T_d, 1%) are about 290°C for DGEBA and 300°C for OC composites. The lowest initial mass loss temperature was observed for OG-PACM-11 composites at about 200°C as shown in Figure 4. This extremely low temperature is probably due to excess unreacted PACM in the sample, which evaporates at lower temperatures. The reactivity of the epoxy ring in OG is higher than that in OC, therefore more secondary amine can react with OG. Although the epoxy/amine ratios are same in the OG and OC composites, more residual PACM molecules exist in the OG sample. A significant mass loss (5%) occurred at temperatures higher than 330°C for all the composites. Table III lists decomposition temperatures and char yields of the composites. The theoretical char yields are calculated from POSS core and eight O—Si attached to the vertexes ($8SiO_{1.5}$ + 8SiO). The char yields at 800°C under N_2 are a little higher than the theoretical values, because the carbon remains in the black residue.

Dynamic mechanical analysis

The moduli of the composites from room temperature to 200°C were evaluated by dynamic mechanical anal-

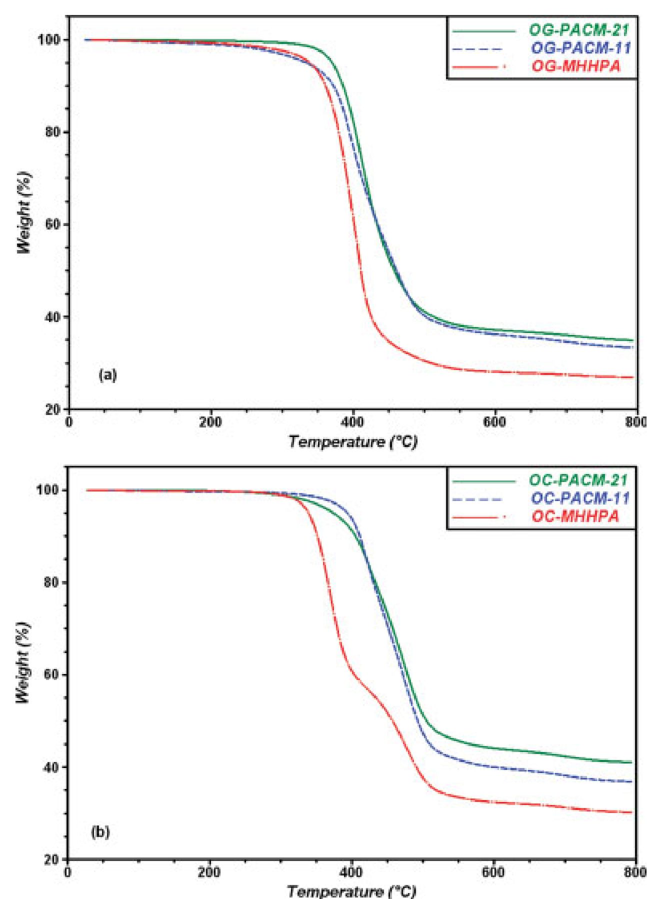

Figure 4 TGA of composites (a) OG, (b) OC. [Color figure can be viewed in the online issue, which is available at www.interscience.wiley.com.]

TABLE III
TGA Results of the Composites

Sample	T_d (1%) (°C)	T_d (5%) (°C)	Char yield (%)	Char yield (theory) (%)
DGEBA-PACM-21	288	332	0.5	0
DGEBA-PACM-11	280	334	0.5	0
DGEBA-MHHPA	291	351	4.4	0
OG-PACM-21	318	370	34.9	32.7
OG-PACM-11	206	335	33.3	27.7
OG-MHHPA	239	339	26.9	25.0
OC-PACM-21	297	373	31.0	31.6
OC-PACM-11	330	394	36.9	27.0
OC-MHHPA	298	339	30.2	24.4

ysis (DMA). Figure 5 shows the DMA graphs of the composites and the modulus values at 30 and 200°C and the glass transition temperature, T_g, taken as the peak temperature in tan δ curves as presented in Table IV. The moduli of DGEBA resins decrease gradually with temperature increasing below T_g and drop rapidly during glass transition to a lowest value. DGEBA-PACM-21 resin, in which one amine reacted with two epoxy, possesses high crosslinking structure and shows higher T_g and modulus than DGEBA-PACM-11. The thermal and mechanical properties of PACM cured DGEBA resin had been investigated over a wide range of epoxy-amine stoichiometry.[17,18] The storage moduli of DGEBA resins in this study are within the range of literature values.

The storage moduli of OG and OC composites at 30°C are close to the values of DGEBA resins. However, the changes in moduli with temperature for the POSS composites are different from the DGEBA resins. The glass transitions were not obvious for most POSS composites. The storage moduli of POSS composites decrease slowly with increases in temperature. OG-PACM-11, OG-MHHPA, and OC-PACM-21 show wider peaks than DGEBA resins in tan δ and loss modulus (not shown) curves. There is no obvious peak in the tan δ curves for other POSS composites. The T_g of OG composites from DMA are about 30–50°C lower than corresponding DGEBA resins, which can be attributed to the more flexible glycidyl propyl ether groups in OG.

The storage moduli of POSS composites at high temperatures are much higher than that of the DGEBA resins. The modulus of OC-PACM-11 is two orders of magnitude higher than that of the corresponding DGEBA resin. The highest modulus at 200°C, 830 MPa, was found for OC-MHHPA. It is not reasonable to compare the modulus simply from the structure difference between POSS and DGEBA. DGEBA resins are rubbery at high temperatures; however, there is no clear glass transition for OC composites below 200°C. In another words, the POSS composite is not a simple polymer structure, which shows distinct glass to rubber state transitions. The

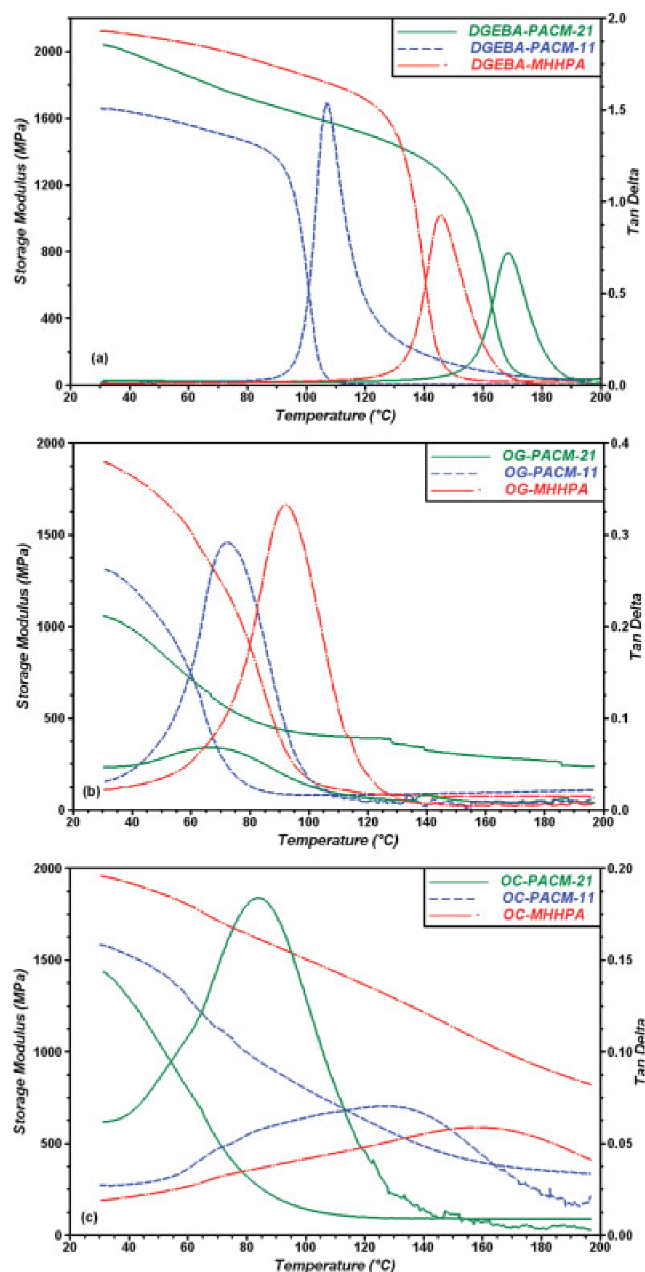

Figure 5 Storage modulus and tan δ of composites (a) DGEBA, (b) OG, and (c) OC. [Color figure can be viewed in the online issue, which is available at www.interscience.wiley.com.]

TABLE IV
Thermal and Mechanical Properties of Composites

Sample	Storage moduli (GPa)		T_g (°C)			CTE (μm/m/°C)	
	30°C	200°C	DMA	DSC	TMA	α_1	α_2
DGEBA-PACM-21	2.0 ± 0.1	0.037 ± 0.001	169	157	163	78 ± 6	170 ± 3
DGEBA-PACM-11	1.7 ± 0.1	0.003 ± 0.001	107	99	104	81 ± 3	225 ± 13
DGEBA-MHHPA	2.1 ± 0.2	0.023 ± 0.002	146	135	145	72 ± 2	190 ± 3
OG-PACM-21	1.0 ± 0.1	0.24 ± 0.03	na	na	na	148 ± 2	na
OG-PACM-11	1.4 ± 0.1	0.12 ± 0.01	72	na	70	129 ± 5	181 ± 2
OG-MHHPA	1.8 ± 0.1	0.070 ± 0.008	92	na	92	110 ± 5	185 ± 9
OC-PACM-21	1.5 ± 0.1	0.091 ± 0.001	84	na	85	126 ± 8	171 ± 4
OC-PACM-11	1.7 ± 0.2	0.32 ± 0.03	na	na	na	128 ± 6	na
OC-MHHPA	2.0 ± 0.1	0.83 ± 0.02	na	na	na	92 ± 5	na

na, not observed.

molecular level mixing/grafting of inorganic phase and organic phase in POSS composites give them different thermal mechanical behavior from the pure polymer. The less temperature dependent moduli and high moduli at high temperatures indicate that POSS composites have potential applications in temperature variable and high temperature environment.

Thermal expansion

The thermal expansion behaviors of the composites were examined by TMA. To observe the temperature dependence of CTE of the composites, the normal dimension change-temperature curves are converted to CTE-temperature curves by taking the derivative to temperature, as shown in Figure 6. DGEBA resins show irregular dimension change near T_g, that decrease slightly first and then increase again. Therefore, their CTE-temperature curves around T_g region are distorted badly after temperature derivative. The two flat regions in the curve represent a smaller CTE value (α_1) below T_g and a higher CTE (α_2) above T_g, respectively.

The thermal expansion behaviors of POSS composites are different from DGEBA resins. TMA of POSS composites show nearly straight lines of dimension change-temperature curve over the measured temperature range. After temperature derivative, OG-PACM-11, OG-MHHPA, and OC-PACM-21 show step-like CTE change near T_g, while OG-PACM-21, OC-PACM-11, and OC-MHHPA show very slow increases in CTE with temperature. The different thermal expansion behaviors of POSS composites are in accordance with the earlier DMA results. The average CTEs of POSS composites over the flat region are calculated from the dimension change over temperature difference and listed in Table IV. It is noteworthy that the observed CTEs above T_g (α_2) of OG-PACM-11, OG-MHHPA, and OC-PACM-21 slightly decrease with temperature, which are different from DGEBA resins that show constant α_2 above T_g. Although DGEBA resins show lower CTEs than POSS composites, their CTE values at rubbery state are 2–3 times of that at glassy state. The large CTE change near T_g may result in large stress. The CTE changes with temperature of POSS composites are small, especially for those samples without glass transition. This is a very useful characteristic of the material for application in temperature variable environment.

Although there is highly crosslinked structure in the POSS composites, the composites do not show lower CTE than corresponding DGEBA resins (α_1). The flexible aliphatic group attached to POSS core, such as glycidyl propyl ether, may be the reason for the high CTEs of OG composites. Instead of glycidyl ether groups with more rigid cyclohexenyl epoxides, OC composites showed smaller CTE than OG composites. Sulaiman et al. reported POSS composites with CTE of 20–30 μm/m/°C, made from a multifunctional epoxy resin cured by OAPS, however, OG and OC composites always showed CTE larger than 100 μm/m/°C even it was cured by OAPS.[16]

Current commercial underfills for electronic packaging are epoxy based composites with silica fillers. They exhibit low CTEs (<40 μm/m/°C is preferred) below T_g. However, when temperature is higher than T_g, the CTEs of underfills will increase dramatically. The applications of such underfills in high temperature environment or high power consuming electronics are limited. As the T_g of the silica-epoxy composites are only slightly affected by the micron sized filler loading,[19] it is anticipated that the CTEs of POSS composites can be reduced by adding silica fillers while still keeping its less temperature dependent CTE characteristics. Figure 7 shows the TMA of silica filled OC-MHHPA composite and no obvious glass transition. The average CTE of the composite is reduced from 92 to 65 μm/m/°C by adding 40 wt % of 3 μm silica. The lower CTE of POSS composites can be obtained by increasing the filler loading. Sulaiman et al. also shows that 10% CTE drops can be reached by adding 10 wt % alumina particles in POSS composites.[16]

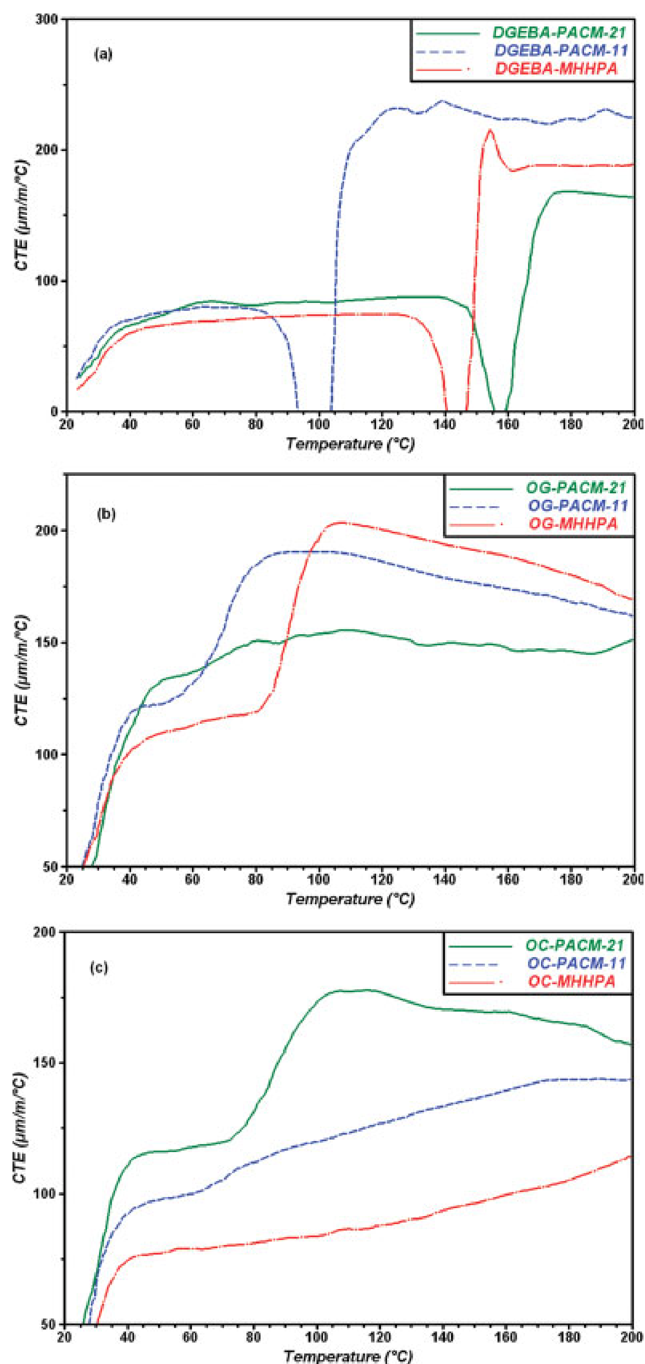

Figure 6 Coefficient of thermal expansion of composites (a) DGEBA, (b) OG, and (c) OC. [Color figure can be viewed in the online issue, which is available at www.interscience.wiley.com.]

Glass transition temperature

The glass transition temperature is an important characteristic of the composite network structure. Three different techniques: modulated DSC, DMA, and TMA were applied to investigate the glass transition behavior. In DSC measurement T_g is defined as the temperature where step-like transition occurs in reverse heat flow curve. T_g is also obtained from the peak temperature in tan δ curve in DMA measurements. When sample shows step-like CTE change in TMA measurement, the T_g is defined as the transition temperature in the dimension change curve. The close T_g values are obtained from different techniques and listed in Table IV.

DGEBA resins show typical glass transitions in DSC, DMA, and TMA measurements. DGEBA-PACM-21 has higher crosslinking structure and shows higher T_g than DGEBA-PACM-11 as expected. The glass transition behavior of POSS composites are more complicated. The glass transitions were not observed for all POSS composites in DSC measurement. In DMA measurement, only OG-PACM-11, OG-MHHPA, and OC-PACM-21 composites show peak in tan δ curve, while the other POSS composites show very broad peaks that are not like the glass transition behavior of normal polymer materials. Similar glass transition behaviors were observed in TMA measurements. OG-PACM-11, OG-MHHPA, and OC-PACM-21 show clear step-like CTE change with temperature, while OG-PACM-21, OC-PACM-11, and OC-MHHPA only show a slightly continuous CTE increase with temperature increasing.

The unusual glass transitions of POSS composites can be attributed to their highly crosslinked structure. OG and OC are octafunctional epoxy and form high crosslinked network throughout the sample. Therefore, the movement of main polymer framework is frozen, and the relaxation can only be reached through the motion of the tether between POSS cores. The tether length (about 22–30 chemical bonds) and property are determined by both hardener and substitute group on POSS. Laine and coworkers analyzed the network tether architectures of OG/DDM and OC/DDM composites, and discussed the nanostructure-macroscopic property relationships.[11] OG has more flexible glycidyl ether groups and shows obvious glass transition. This is also the reason that

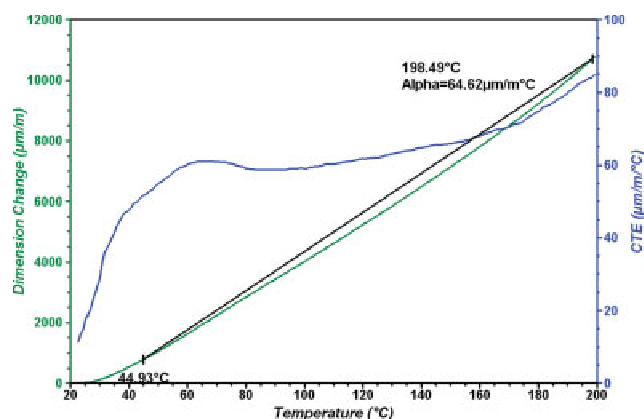

Figure 7 CTE of OC-MHHPA composite containing 40 wt % of silica (3 μm). [Color figure can be viewed in the online issue, which is available at www.interscience.wiley.com.]

T_gs of OG composites are 30–50°C lower than corresponding DGEBA resins. When the tether is fixed by further crosslinking through the reaction of secondary amine as in OG-PACM-21, tether motion will be hindered and the glass transition disappeared. OC has more rigid and cyclic groups than OG and the tether motion requires more energy. The slight tether motion is not enough to cause relaxation of the composite. The observed glass transition for OC-PACM-21 is probably due to the incomplete reaction between epoxy and secondary amine group as discussed earlier, which reduces the crosslink density and causes defects in the sample.

CONCLUSIONS

POSS epoxy hybrid composites have very high crosslinking densities and show unique thermal and mechanical properties. The thermochemical and FTIR data indicate that the curing reactions of POSS composites are difficult because of the steric hindrance, so the high curing temperatures are required. Aliphatic amine and anhydride hardener can cure POSS epoxy efficiently. Anhydride cured POSS epoxy composites show higher moduli and lower CTEs than the corresponding amine cured samples. The high crosslinking through eight vertexes on POSS cores make the motion of main polymer framework frozen, and the apparent relaxations of the POSS composites are probably through the motions of tethers between POSS cores. Therefore, POSS composites do not show obvious glass transition as normal epoxy resins. Their storage moduli and thermal expansions are less dependent on the temperature. The high moduli and low CTEs at high temperatures make POSS composites potential candidates for applications in high temperature and temperature variable environments.

References

1. Zhang, Z. Q.; Wong, C. P. IEEE Trans Adv Packag 2004, 27, 515.
2. Sun, Y. Y.; Zhang, Z. Q.; Wong, C. P. IEEE Trans Comp Packag Technol 2006, 29, 190.
3. Laine, R. M. J Mater Chem 2005, 15, 3725.
4. Agaskar, P. A. Inorg Chem 1990, 29, 1603.
5. Sellinger, A.; Laine, R. Chem Mater 1996, 8, 1592.
6. Laine, R. M.; Choi, J. W.; Lee, I. Adv Mater 2001, 13, 800.
7. Lee, L.; Chen, W. Polymer 2005, 46, 2163.
8. Neumann, D.; Fisher, M.; Tran, L.; Matisons, J. J Am Chem Soc 2002, 124, 13998.
9. Toepfer, O.; Neumann, D.; Choudhury, N.; Whittaker, A.; Matisons, J. Chem Mater 2005, 17, 1027.
10. Lee, Y. J.; Kuo, S. W.; Huang, C. F.; Chang, F. C. Polymer 2006, 47, 4378.
11. Choi, J.; Yee, A. F.; Laine, R. M. Macromolecules 2003, 36, 5666.
12. Choi, J.; Harcup, J.; Yee, A. F.; Zhu, Q.; Laine, R. M. J Am Chem Soc 2001, 123, 11420.
13. Chen, W.; Wang, Y.; Kuo, S.; Huang, C.; Tung, P.; Chang, F. Polymer 2004, 45, 6897.
14. Lee, Y.; Huang, J.; Kuo, S.; Lu, J.; Chang, F. Polymer 2005, 46, 173.
15. Huang, J. C.; He, C. B.; Liu, X. M.; Xu, J. W.; Tay, C. S. S.; Chow, S. Y. Polymer 2005, 46, 7018.
16. Sulaiman, S.; Brick, C. M.; De Sana, C. M.; Katzenstein, J. M.; Laine, R. M.; Basheer, R. A. Macromolecules 2006, 39, 5167.
17. Vanlandingham, M. R.; Eduljee, R. F.; Gillespie, J. W. J Appl Polym Sci 1999, 71, 699.
18. Skourlis, T. P.; McCullough, R. L. J Appl Polym Sci 1996, 62, 481.
19. Sun, Y. Y.; Zhang, Z. Q.; Moon, K. S.; Wong, C. P. J Polym Sci Part B: Polym Phys 2004, 42, 3849.